Integrative and Comparative Biology

Integrative and Comparative Biology, volume 62, number 3, pp. 652–667
https://doi.org/10.1093/icb/icac021

Society for Integrative and Comparative Biology

SYMPOSIUM

Evolutionary Patterns in Chemical Composition and Biomechanics of Articulated Coralline Algae

Kyra G. Janot [*,1], Faride Unda [†], Shawn D. Mansfield [†] and Patrick T. Martone [*]

[*]Department of Botany and Biodiversity Research Centre, University of British Columbia, 6270 University Blvd., Vancouver, BC V6T 1Z4, Canada; [†]Department of Wood Science, University of British Columbia, 2424 Main Mall, Vancouver, BC V6T 1Z4, Canada

From the symposium "Evolutionary patterns in chemical composition and biomechanics of joints in wave-swept, segmented seaweeds" presented at the annual meeting of the Society for Integrative and Comparative Biology, January 3-7, 2022, at Phoenix, Arizona.

[1]Email: kjanot@gmail.com

Synopsis Seaweeds inhabiting wave-battered coastlines are generally flexible, bending with the waves to adopt more streamlined shapes and reduce drag. Coralline algae, however, are firmly calcified, existing largely as crusts that avoid drag altogether or as upright branched forms with uncalcified joints (genicula) that confer flexibility to otherwise rigid thalli. Upright corallines have evolved from crustose ancestors independently multiple times, and the repeated evolution of genicula has contributed to the ecological success of articulated corallines worldwide. Structure and development of genicula are significantly different across evolutionary lineages, and yet biomechanical performance is broadly similar. Because chemical composition plays a central role in both calcification and biomechanics, we explored evolutionary trends in cell wall chemistry across crustose and articulated taxa. We compared the carbohydrate content of genicula across convergently evolved articulated species, as well as the carbohydrate content of calcified tissues from articulated and crustose species, to search for phylogenetic trends in cell wall chemistry during the repeated evolution of articulated taxa. We also analyzed the carbohydrate content of one crustose coralline species that evolved from articulated ancestors, allowing us to examine trends in chemistry during this evolutionary reversal and loss of genicula. We found several key differences in carbohydrate content between calcified and uncalcified coralline tissues, though the significance of these differences in relation to the calcification process requires more investigation. Comparisons across a range of articulated and crustose species indicated that carbohydrate chemistry of calcified tissues was generally similar, regardless of morphology or phylogeny; conversely, chemical composition of genicular tissues was different across articulated lineages, suggesting that significantly different biochemical trajectories have led to remarkably similar biomechanical innovations.

Introduction

Corallines are a group of calcifying red algae that display a wide array of morphologies, from crustose forms to upright branching fronds (Fig. 1). These different morphologies have distinct biomechanical implications for species that live on wave-swept rocky shores, where they contend with significant hydrodynamic stress in the form of drag (Steneck 1986). Most macroalgae withstand drag by being flexible, which allows them to bend over and reconfigure into smaller more streamlined shapes (Denny and Gaylord 2002; Harder et al. 2004; Boller and Carrington 2006; Martone et al. 2012); corallines, however, are composed mostly of calcified tissues that result in a rigid thallus (Johansen 1981). This does not pose a problem for crustose forms that generally avoid drag by lying flat and attaching completely to the substrate. Upright corallines, in contrast, survive wave action by possessing uncalcified articulations ("genicula") that separate calcified segments ("intergenicula"), allowing

Advance Access publication April 28, 2022

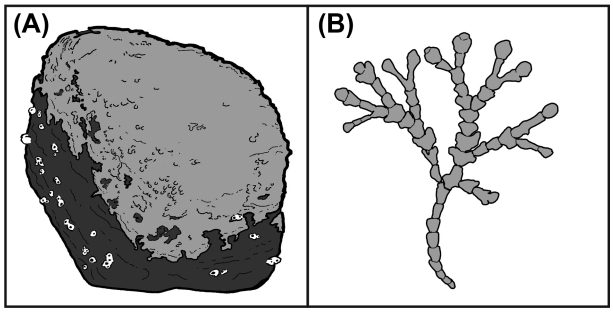

Fig. 1 Illustrated example of a crustose coralline on a rock (**A**) and an upright articulated coralline frond (**B**).

otherwise rigid fronds to be flexible. This flexibility is critical to the survival and success of upright corallines in wave-swept habitats.

Different structures, same function

Despite the advantages conveyed by genicula, achieving flexibility through segmentation has mechanical consequences, as limiting bending to discrete joints concentrates stress at those joints (Martone and Denny 2008; Janot and Martone 2018). The evolution of genicula represents a trade-off between increasing flexibility to bend, while decreasing or withstanding the concentrated stress. Both the fossil record and molecular data indicate that this balancing act has occurred not just once, but at least three separate times, with upright articulated corallines evolving independently from crustose ancestors in three different subfamilies within the Corallinales: Corallinoideae, Lithophylloideae, and Metagoniolithoideae (Bailey and Chapman 1998; Aguirre et al. 2010; Bittner et al. 2011; Kato et al. 2011; Kundal 2011). Genicula are, therefore, analogous across the three lineages, as they allow otherwise rigid coralline structures to bend without breaking, but they are not homologous—rather, they represent a clear case of convergent evolution.

Genicula from the three articulated clades (see Fig. 2) achieve flexibility in somewhat different ways. Corallinoid fronds have a great number of short genicula that are at increased risk of stress amplification, but are composed of tissues that are both stronger and tougher than the tissues in other articulated groups; lithophylloid fronds have fewer genicula, but are composed of particularly extensible tissues; metagoniolithoid fronds have very long genicula and short intergenicula, allowing them to achieve higher flexibilities than either corallinoids or lithophylloids (Janot and Martone 2018). Differences in genicular morphology may be the result of different developmental or structural constraints, as genicular initiation and cellular organization are distinct within each subfamily (Johansen 1969, 1981; Ducker 1979). At the same time, differences in material properties may offset the consequences of morphologies that are at greater risk of stress amplification or are inherently less flexible (Janot and Martone 2016, 2018).

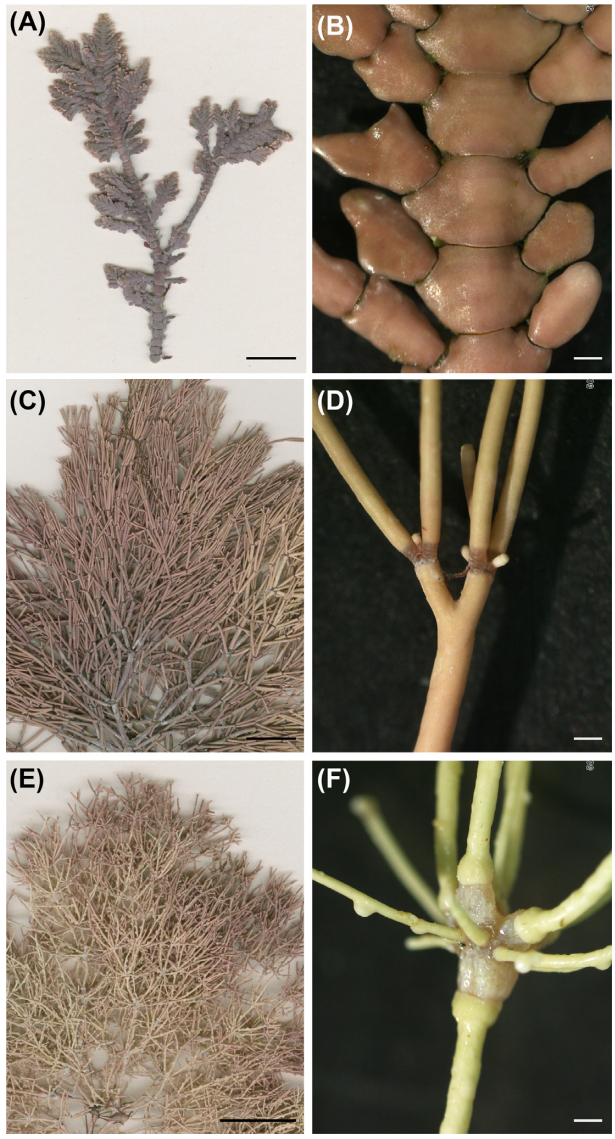

Fig. 2 Representative articulated coralline thalli and genicula from the three subfamilies. (**A**) and (**B**) *Johansenia macmillanii*, Corallinoideae (UBC A91561), (**C**) and (**D**) *Amphiroa gracilis*, Lithophylloideae (UBC A91572), and (**E**) and (**F**) *Metagoniolithon* sp. 1, Metagoniolithoideae (UBC A91581). Scale = 1 cm in (**A**), (**C**), and (**E**); scale = 500 um in (**B**), (**D**), and (**F**).

Chemical composition of genicula

The polysaccharide composition of algal cell walls impacts their material properties (Rees and Conway 1962; Kloareg and Quatrano 1988; Kraemer and Chapman 1991; Carrington et al. 2001; Martone et al. 2010; Starko et al. 2018), yet little is known about the chemical composition of independently derived genicula within

articulated coralline clades. Several studies have investigated the chemical composition of corallinoids (Turvey and Simpson 1965; Okazaki et al. 1982; Cases et al. 1992, 1994; Usov et al. 1995, 1997; Takano et al. 1996; Navarro and Stortz 2002, 2008; Martone et al. 2010, 2019), but work on articulated lithophylloids has been limited to the investigation of alginic acids (Okazaki and Tazawa 1989; Bilan and Usov 2001) and metagoniolithoid chemistry has been completely ignored. Furthermore, most studies have been performed on combined genicular and intergenicular tissues or on crusts (but see Martone et al. 2010), so even less is known specifically about genicular chemistry. If genicular chemistry is similar across subfamilies, then it may suggest that the repeated evolution of genicula involves the activation of similar biochemical pathways, despite differences in development. If genicular chemistry is different across subfamilies, which seems likely given the inherent differences in material properties (Janot and Martone 2016), then results would underscore the different evolutionary trajectories that have led to surprisingly similar structures in each subfamily.

Like other red algae, corallines possess cell walls composed of cellulose microfibrils embedded within an amorphous matrix of sulfated galactans and glycoproteins (Frei and Preston 1961; Kloareg and Quatrano 1988). While most non-coralline red algal tissues contain between 1 and 8% cellulose by dry weight (Kloareg and Quatrano 1988), genicula of the corallinoid *Calliarthron tuberculosum* contain ~15% (Martone et al. 2019) and—perhaps consequently—have a higher tensile strength than non-coralline reds (Hale 2001; Martone 2006; Janot and Martone 2016; Martone et al. 2019). Cellulose content has been linked to tensile strength in terrestrial plants (Girault et al. 1997; Genet et al. 2005; Burgert 2006) and at least one marine alga (Starko et al. 2018), so we hypothesize that species with stronger genicular tissues also contain more cellulose.

Sulfated galactans may impact mechanical properties such as strength, extensibility, and stiffness (Rees and Conway 1962; Carrington et al. 2001). Sulfated galactans are a family of polymers with a backbone of alternating β-1,3 galactose and α-1,4 galactose (or its 3,6 anhydro derivative). While the β-galactose units are always in the D configuration, the α-galactose units may be in the D-configuration (carrageenans) or the L-configuration (agarans), and galactans synthesized by corallines fall primarily into the latter category (Cases et al. 1992, 1994; Takano et al. 1996; Usov et al. 1997; Navarro and Stortz 2002, 2008; Martone et al. 2010). Various combinations of O-linked groups such as sulfate esters, methyl ethers, or xylose and galactose side chains may also be attached to the galactan backbone, leading to a range of gelling properties (Kloareg and Quatrano 1988; Usov 1992; Bilan and Usov 2001; Navarro and Stortz 2002, 2008). Based on differences in material properties, we hypothesize that genicular tissues of corallinoids, lithophylloids, and metagoniolithoids contain different combinations of galactan side chains, as well as different total galactan content.

Chemical composition of calcified tissues

One major limitation of most published work on coralline cell wall chemistry has been the failure to analyze tissue types separately. While this is not an issue when studying crustose species, it is likely that genicular and intergenicular tissue of articulated corallines differ in their chemical composition. Indeed, Martone et al. (2010) found significant differences in the structure of galactans found in genicula and intergenicula of *Calliarthron cheilosporioides*. Specifically, galactans found in *Calliarthron* intergenicula had low levels of O-methylation and high amounts of xylosyl side branches on C-6 of the β-galactose units, while galactans found in *Calliarthron* genicula had high O-methylation and only minor amounts of xylosyl side branching. Xylogalactans with a ratio of roughly 1:3 xylose:galactose have been found in both articulated and crustose coralline species (Turvey and Simpson 1965; Cases et al. 1992, 1994; Usov et al. 1995, 1997; Takano et al. 1996; Navarro and Stortz 2002, 2008; Navarro et al. 2011), suggesting that xylosyl side branches maybe involved in the calcification process.

Given that calcification is an ancestral trait across coralline algae, we hypothesize that the chemical composition of calcified tissues (crusts and intergenicula) is similar. If xylogalactans are involved in calcification, then we expect them to be abundant in all calcified coralline tissues regardless of thallus morphology or evolutionary history, and rare in genicular tissues. At the same time, we hypothesize that overall chemical composition of calcified tissues will reflect evolutionary history rather than thallus morphology (i.e., intergenicula of a given articulated group will be more chemically similar to closely related crusts than to intergenicula of other articulated groups).

In this study, we compared the monosaccharide composition of tissues from seven articulated coralline species and four crustose coralline species to test whether chemical composition reflects tissue type, thallus morphology, evolutionary history, or material properties. We also performed linkage analysis on genicular tissues from select articulated species to broadly characterize and compare polysaccharide

structure. By separately analyzing genicula and intergenicula of articulated species, as well as tissues from crustose species, we were able to look for chemical differences between uncalcified and calcified tissues that might be linked to the calcification process. By analyzing crustose species that are closely related to each articulated clade—including one corallinoid crust that evolved from articulated ancestors and represents an "evolutionary reversal" (Hind et al. 2018)—we were also able to investigate whether calcified tissues from articulated taxa bear chemical resemblance to tissues of closely related crusts, or whether intergenicula are consistently chemically distinct from crustose tissues. Finally, by comparing the chemical composition of genicula from the three articulated clades, we explored the role of polysaccharides in determining the material properties of these mechanically critical structures.

Materials and methods

Specimen collection

Species from subfamily Corallinoideae (*C. tuberculosum*, *Corallina chilensis*, and *Johansenia macmillanii*) were collected from Botanical Beach on Vancouver Island, BC, Canada. Articulated species from subfamily Lithophylloideae (*Amphiroa* sp. and *Amphiroa gracilis*) and two species from subfamily Metagoniolithoideae (*Metagoniolithon stelliferum* and *Metagoniolithon* sp.1) were collected from Point Peron, Perth, Western Australia. *Metagoniolithon* sp.2 was collected off Carnac Island near Perth, Western Australia. Representative vouchers for each species were deposited into the University of British Columbia Herbarium for future taxonomic reference (see collection details in Supplementary Table S1).

Crustose species were selected based on phylogenetic position relative to articulated clades: *Lithophyllum* sp. (Lithophylloideae) is closely related to the articulated clade within Lithophylloideae, *Chamberlainium tumidum* (Porolithoideae) is within a subfamily that is relatively closely related to the entirely articulated Metagoniolithoideae, *Neogoniolithon frutescens* (Neogoniolithoideae) is within a subfamily that is relatively closely related to the mostly articulated Corallinoideae, and *Bossiella mayae* is a crustose species nested within the Corallinoideae (Bailey and Chapman 1998; Aguirre et al. 2010; Bittner et al. 2011; Kato et al. 2011; Kundal 2011; Hind et al. 2018). *Lithothamnion* sp. (Melobesioideae) was selected as a crustose representative of the order Sporolithales, which is sister to the order Corallinales that contains all articulated clades. Specimens of *C. tumidum* and *Lithothamnion* sp. were collected intertidally from West Beach Boulders on Calvert Island, BC, Canada. *Lithophyllum* sp. and *B. mayae* specimens were collected intertidally from North Beach Bench on Calvert Island. Specimens of the rhodolith-forming species *N. frutescens* were collected subtidally from Moorea, French Polynesia. Representative vouchers for each species were deposited into the University of British Columbia Herbarium for future taxonomic reference (see collection details in Supplementary Table S1).

Species determinations

DNA was extracted from a subset of specimens of each morphologically identified species following Saunders and McDevit (2012), except for *C. tuberculosum* and *J. macmillanii*, specimens of which have been previously sequenced from the same populations. Gene fragments of mitochondrial cytochrome c oxidase subunit (CO1, 664 bp) or photosystem II protein D1 (psbA, 851 bp) were amplified following Hind et al. (2016), sequenced, edited, and aligned with Geneious Prime 2021.2.2 (Kearse et al. 2012), and then compared against sequences in GenBank (Sayers et al. 2020), BOLD (The Barcode of Life Data System; Ratnasingham and Hebert 2007), and a local database using BLAST (Basic Local Alignment Search Tool; Altschul et al. 1997; see Supplementary Table S1). Species names were applied where possible, and genus names were applied when no matches (> 99% similarity) were found to previously published sequences with accepted names.

Tissue preparation

Both articulated and crustose species were inspected carefully for epiphytes, which were removed manually with either forceps or a toothbrush. Only healthy (i.e., brightly pigmented, hydrated, and fully intact) vegetative tissues were used. Specimens were dried *via* plant press (for articulated species) or silica gel (for crustose species), and intergenicula and genicula of articulated species were carefully separated using a razor blade under a dissecting microscope. In order to minimize cross-contamination of tissues, genicular and intergenicular segments were trimmed to exclude the zone where tissue types meet. Tissues were macerated with a mortar and pestle, after which calcified tissues were decalcified *via* dropwise addition of 1 M HCl and constant stirring until no residual bubbling was detected. Decalcified tissues were centrifuged at 10,000 rpm for 5 min, and the supernatant was removed and discarded. Decalcified pellets of intergenicula and crustose tissues, as well as macerated genicular tissues, were dried for 48 h in an oven at 50°C. Decalcified tissues were reground in a mortar and pestle following

oven drying, then placed back in the oven for a minimum of 1 h prior to weighing for acid hydrolysis.

Monosaccharide composition analysis

A scaled-down modification of the secondary acid hydrolysis was performed on all tissues (Huntley et al. 2003). In brief, samples of ~1 mg of genicular/intergenicular tissue or ~10 mg of crustose tissue were weighed out into 2 mL graduated, free-standing microcentrifuge tubes with screw-caps and o-rings (catalog #02–681–374, ThermoFisher Scientific, Waltham, MA). These tubes were used because of their slightly > 2 mL capacity, which was necessary for the following procedure. A volume of 50 μL of 72% H_2SO_4 was added to ~1 mg of ground tissue (articulated species), or 100 μL was added to ~10 mg of ground tissue (crustose species). Samples were vortexed briefly, then incubated in a heating block at 30°C for 1 h while being shaken at 500 rpm. A volume of 1 mL (for 1 mg samples) or 2 mL (for 10 mg samples) of deionized H_2O was added, and samples were vortexed briefly to resuspend tissue. Samples were then autoclaved at 121°C for 60 min, allowed to cool, and centrifuged at 13,000 rpm for 10 min. The supernatant was separated from the remaining pellet, then filtered through 0.45 μm syringe filters. Filtered supernatants were analyzed for monosaccharide composition using a high-performance liquid chromatograph (HPLC; Dionex DX-600, ThermoFisher Scientific) with an ion exchange PA-1 column and a Dionex AS-50 autosampler (ThermoFisher Scientific). Samples were injected in 25 μL volumes onto the column and eluted with deionized H_2O at a rate of 1 mL/min, followed by post-column addition of 200 mM NaOH at 0.5 mL/min prior to detection by pulsed amperometry. All samples were run with technical duplicates. Neutral sugar standards containing glucose (Glu), galactose (Gal), xylose (Xyl), fucose (Fuc), arabinose (Ara), rhamnose (Rha), and mannose (Man) were subjected to the same procedure and analyzed by HPLC alongside tissue samples to account for monosaccharide breakdown.

For articulated species, each sample represented a unique pooled set of three to five individuals, due to the minimal weight of genicula and decalcified tissues. For crustose species, each sample represented tissue from a single individual. For most species, five samples per tissue type were prepared (i.e., five genicular and five intergenicular samples per articulated species and five samples total for each crustose species). As only four specimens of *Lithothamnion* sp. were successfully collected, only four samples were prepared for this species.

Linkage analysis

Linkage analysis of carbohydrates was performed by the Complex Carbohydrate Research Center at the University of Georgia, using a protocol modified from Heiss et al. (2009). In order to be analyzed, samples first had to be desulfated. Approximately 1 mg samples of ground genicular tissue from *C. tuberculosum*, *A. gracilis*, and *Metagoniolithon* sp.1 were sonicated and heated in water to dissolve soluble material, after which sulfated polysaccharides were converted to pyridinium salts using DOWEX resin activated with 10% pyridine. Samples were filtered through glass wool to remove the resin and insoluble material, and soluble material was suspended in a heated mixture of dimethyl sulfoxide (DMSO) and methanol to remove the sulfate groups. After removal of DMSO, samples underwent a series of steps involving permethylation, reduction, repermethylated depolymerization, reduction, and acetylation as described in Heiss et al. (2009), and the resulting partially methylated alditol acetates were analyzed *via* gas chromatography-mass spectrometry (Hewlett-Packard 5890 GC, Hewlett-Packard, Palo Alto, CA). Potential structural units were assigned to linkages where possible, based on what has previously been found in corallines (Turvey and Simpson 1965; Okazaki et al. 1982; Cases et al. 1992, 1994; Usov et al. 1995, 1997; Takano et al. 1996; Navarro and Stortz 2002, 2008; Martone et al. 2010; Navarro et al. 2011).

Multivariate comparisons between tissue types and subfamilies

Principal components analysis (PCA) was performed on neutral monosaccharide data in R (version 4.1.1, R Core Team 2021) using the RStudio interface (version 2021.09.0, RStudio Team 2021) and the PCA() function in the FactoMineR package (version 2.4, Husson et al. 2008). All data were log transformed and scaled to avoid disproportionate effects of more abundant monosaccharides. PCAs were performed first on all neutral monosaccharide data for all tissue types to determine whether calcified tissues from articulated and crustose species were more similar than either tissue type compared to genicular tissues. PCAs were then performed on calcified tissues alone (i.e., intergenicula and crusts) and genicular tissues alone to look for separation based on phylogeny. Using the Kaiser criterion, only principal components with eigenvalues > 1 were considered further. For further qualitative analysis, the fviz_pca_ind() function in the factoextra package (version 1.0.7, Kassambara and Mundt 2020) was used to draw 95% confidence intervals around subfamilies and tissue types.

Permutational multivariate analyses of variance (PERMANOVA) were performed on different models for each data set. The model for all data included calcification as a factor, the model for genicular tissues included subfamily as a factor, and the model for calcified tissues included tissue type (intergenicula vs crust), clade (articulated subfamilies and their most closely related crusts), and the interaction as factors. PERMANOVA's were run in RStudio using the adonis() function from the vegan package (version 2.5.7, Oksanen et al. 2020). Homogeneity of multivariate dispersion was tested using the betadisper() function in the vegan package.

Phylogenetic signal analysis

In order to investigate the importance of evolutionary history on the chemical composition of calcified coralline tissues, measurements of phylogenetic signal were calculated for both monosaccharide data and principal components from a PCA run only on calcified tissues. CO1 sequences were edited and aligned in Geneious Prime, and a maximum likelihood (ML) analysis was performed in MEGA (version 11.0.8, Kumar et al. 2018) using the GTR + I + G model of evolution as determined by jModelTest (version 2.1.10, Darriba et al. 2012) with 500 bootstrap replicates. In instances where CO1 sequences were not successfully obtained from specimens collected for this study, species identity was confirmed with psbA (with the exception of *C. tuberculosum* and *J. macmillanii*) and the corresponding CO1 sequences were downloaded from either a local database or GenBank. One exception was *Lithothamnion* sp., which had a CO1 sequence that did not match any sequence in any database—therefore, a CO1 sequence from the closely related species *Lithothamnion glaciale* was used. The resulting phylogeny was used to calculate Blomberg's κ and Pagel's λ in RStudio with the phylosig() function in the phytools package (version 0.7.90, Revell 2012). Blomberg's κ and Pagel's λ were calculated for all principal component axes that resulted from analysis of calcified tissues, as well as for individual monosaccharides.

Correlating monosaccharides with biomechanical properties

In order to gain a preliminary understanding of the relationship between chemistry and genicular mechanical properties, we compared species averages of genicular strength (breaking stress, σ, MPa) and extensibility (breaking strain, ε, mm/mm) published in Janot and Martone (2016) with species averages of the most abundant monosaccharides (glucose, galactose, and xylose). Mechanical data was log transformed to meet assumptions of normality and homoscedasticity. Model selection was performed using the glmulti() function in the glmulti package (version 1.0.8, Calcagno 2020). The resulting linear regressions were tested for significance using the anova() function in the base stats package in R.

Results

Monosaccharide composition

Glucose, galactose, and xylose were found in all species and tissue types (Table 1). Mannose was detected in nearly all species and tissues types, but was notably absent from both the genicula and intergenicula of all three *Metagoniolithon* species. Arabinose was absent from all samples and was, therefore, removed from further analyses. Fucose and rhamnose levels varied across species and tissue types, though they never exceeded 1% dry weight when present.

Glucose was the dominant monosaccharide in all calcified tissue, with levels ranging from 1.3 (*M. stelliferum*) to almost 35 (*Lithothamnion* sp.) times higher than the next most abundant monosaccharide, galactose. In corallinoid genicula, glucose was the most abundant monosaccharide present; however, galactose was more abundant than glucose in the genicula of all articulated lithophylloid and metagoniolithoid species. Both galactose and xylose content were consistently higher in genicular tissue than in intergenicular tissue for all articulated species tested, indicating a higher level of galactans in general (Table 1). Crustose tissues were also relatively low in galactose and xylose content. Galactose and xylose were particularly abundant in lithophylloid and metagoniolithoid genicula when compared to corallinoid genicula. The relative proportion of xylose: galactose varied for both genicula and calcified tissues, from 0.02:1 to 1.09:1, with no clear pattern based on either tissue type or phylogeny (Table 2).

Linkage analysis

The genicula of *A. gracilis*, *Metagoniolithon* sp.1, and *C. tuberculosum* all possessed 4-Glu, likely indicating the presence of cellulose (Table 3). Hemicellulosic polysaccharides can also have a backbone of 1,4-Glu, but they are not typically abundant in red algae relative to other polysaccharides (Kloareg and Quatrano 1988; Masarin et al. 2016). The mol% of glucose was much higher overall in *C. tuberculosum* than the other two species, and one linkage (3-Glu) was only found in *Calliarthron*. The source of this linkage is unknown. The total %mol glucose of each species tested *via* linkage analysis was significantly lower than what was seen in the monosaccharide composition analysis, but

Table 1 Monosaccharide composition (% dry weight) of genicular, intergenicular, and crust tissues. All values indicate average ± SEM, $n = 5$, except for *Lithothamnion* sp. ($n = 4$)

			Monosaccharide composition (% dry weight)						
	Subfamily	**Species**	**Glucose**	**Galactose**	**Xylose**	**Fucose**	**Rhamnose**	**Mannose**	**Total**
Genicula	Corallinoideae	*C. tuberculosum*	6.24 ± 0.34	5.98 ± 0.32	0.12 ± 0.01	—	0.02 ± 0.02	0.27 ± 0.03	12.62 ± 0.78
	Corallinoideae	*C. chilensis*	15.38 ± 1.11	2.83 ± 0.20	1.68 ± 0.10	0.10 ± 0.01	0.79 ± 0.05	0.37 ± 0.03	21.14 ± 1.49
	Corallinoideae	*J. macmillanii*	10.30 ± 0.44	5.30 ± 0.28	0.20 ± 0.02	0.16 ± 0.01	0.12 ± 0.01	0.37 ± 0.02	16.46 ± 0.75
	Lithophylloideae	*A. gracilis*	6.17 ± 0.32	10.81 ± 0.42	11.76 ± 0.54	0.32 ± 0.01	0.52 ± 0.02	0.95 ± 0.05	30.53 ± 1.24
	Lithophylloideae	*Amphiroa* sp.	5.49 ± 0.36	11.40 ± 0.61	3.29 ± 0.36	0.16 ± 0.01	0.04 ± 0.01	0.30 ± 0.05	20.68 ± 0.59
	Metagoniolithoideae	*Metagoniolithon* sp.1	1.48 ± 0.08	3.79 ± 0.15	2.80 ± 0.13	0.06 ± 0.01	0.09 ± 0.01	—	8.22 ± 0.32
	Metagoniolithoideae	*Metagoniolithon* sp.2	2.88 ± 0.13	8.06 ± 0.84	4.57 ± 0.44	0.10 ± 0.01	—	—	15.61 ± 1.38
	Metagoniolithoideae	*M. stelliferum*	3.72 ± 0.32	6.85 ± 0.41	2.04 ± 0.13	0.07 ± 0.01	—	—	12.68 ± 0.83
Intergenicula	Corallinoideae	*C. tuberculosum*	19.98 ± 5.65	0.98 ± 0.31	0.05 ± 0.05	0.14 ± 0.02	—	0.20 ± 0.06	21.34 ± 6.01
	Corallinoideae	*C. chilensis*	10.67 ± 0.63	0.61 ± 0.03	0.06 ± 0.01	0.07 ± 0.01	0.02 ± 0.01	0.08 ± 0.02	11.51 ± 0.68
	Corallinoideae	*J. macmillanii*	11.72 ± 0.93	0.76 ± 0.07	0.02 ± 0.01	0.09 ± 0.01	—	0.16 ± 0.01	12.75 ± 1.02
	Lithophylloideae	*A. gracilis*	31.49 ± 3.43	2.22 ± 0.35	0.77 ± 0.26	0.17 ± 0.02	0.13 ± 0.06	0.38 ± 0.05	35.17 ± 4.10
	Lithophylloideae	*Amphiroa* sp.	11.03 ± 1.43	0.88 ± 0.12	0.07 ± 0.01	0.04 ± 0.01	—	0.20 ± 0.01	12.22 ± 1.55
	Metagoniolithoideae	*Metagoniolithon* sp.1	5.60 ± 0.89	1.98 ± 0.34	0.23 ± 0.05	—	0.31 ± 0.24	—	8.12 ± 0.51
	Metagoniolithoideae	*Metagoniolithon* sp.2	15.49 ± 1.07	3.65 ± 0.38	0.55 ± 0.10	0.08 ± 0.01	0.16 ± 0.02	—	19.93 ± 1.03
	Metagoniolithoideae	*M. stelliferum*	5.02 ± 0.58	3.82 ± 0.35	0.28 ± 0.04	0.04 ± 0.01	0.06 ± 0.03	—	9.23 ± 0.76
Crusts	Corallinoideae	*B. mayae*	4.21 ± 0.23	0.12 ± 0.02	0.01 ± 0.01	0.02 ± 0.01	—	00.03 ± 0.01	4.39 ± 0.22
	Neogoniolithoideae	*N. frutescens*	17.07 ± 0.93	2.48 ± 0.30	0.44 ± 0.10	0.09 ± 0.01	0.01 ± 0.01	0.39 ± 0.04	20.48 ± 1.14
	Lithophylloideae	*Lithophyllum* sp.	4.37 ± 0.35	0.27 ± 0.04	0.02 ± 0.01	0.02 ± 0.01	0.03 ± 0.01	0.06 ± 0.01	4.77 ± 0.40
	Chamberlainoideae	*C. tumidum*	7.16 ± 0.69	0.49 ± 0.08	0.05 ± 0.01	0.07 ± 0.01	0.03 ± 0.01	0.28 ± 0.05	8.07 ± 0.85
	Melobesioideae	*Lithothamnion* sp.	3.95 ± 0.76	0.11 ± 0.06	0.02 ± 0.01	0.02 ± 0.01	0.01 ± 0.01	0.06 ± 0.05	4.18 ± 0.87

Table 2 Monosaccharide composition relative to total sugar content (mol%) of genicular, intergenicular, and crust tissues. All values indicate average ± s.e.m., n = 5, except for *Lithothamnion* sp. (*n* = 4)

			Monosaccharide composition (mol%)						Ratios	
	Subfamily	**Species**	**Glucose**	**Galactose**	**Xylose**	**Fucose**	**Rhamnose**	**Mannose**	**Glu:Gal**	**Xyl:Gal**
Genicula	Corallinoideae	*C. tuberculosum*	49.42	47.39	0.92	—	0.17	2.11	1.04:1	0.01:1
	Corallinoideae	*C. chilensis*	72.74	13.37	7.92	0.48	3.72	1.77	5.44:1	0.59:1
	Corallinoideae	*J. macmillanii*	62.59	32.20	1.23	1.00	0.73	2.24	1.94:1	0.04:1
	Lithophylloideae	*A. gracilis*	20.20	35.42	38.53	1.05	1.71	3.10	0.57:1	1.09:1
	Lithophylloideae	*Amphiroa* sp.	26.55	55.14	15.91	0.76	0.20	1.44	0.48:1	0.29:1
	Metagoniolithoideae	*Metagoniolithon* sp.1	18.04	46.11	34.01	0.78	1.07	—	0.39:1	0.74:1
	Metagoniolithoideae	*Metagoniolithon* sp.2	18.44	51.62	29.31	0.63	—	—	0.36:1	0.57:1
	Metagoniolithoideae	*M. stelliferum*	29.33	54.00	16.11	0.55	—	—	0.54:1	0.30:1
Intergenicula	Corallinoideae	*C. tuberculosum*	93.57	4.60	0.24	0.66	—	0.93	20.36:1	0.05:1
	Corallinoideae	*C. chilensis*	92.70	5.33	0.55	0.59	0.15	0.68	17.39:1	0.10:1
	Corallinoideae	*J. macmillanii*	91.88	5.99	0.19	0.69	—	1.25	15.34:1	0.03:1
	Lithophylloideae	*A. gracilis*	89.54	6.32	2.19	0.49	0.37	1.09	14.18:1	0.35:1
	Lithophylloideae	*Amphiroa* sp.	90.26	7.19	0.56	0.37	—	1.61	12.55:1	0.08:1
	Metagoniolithoideae	*Metagoniolithon* sp.1	68.95	24.35	2.87	—	3.83	—	2.83:1	0.12:1
	Metagoniolithoideae	*Metagoniolithon* sp.2	77.71	18.32	2.77	0.38	0.82	—	4.24:1	0.15:1
	Metagoniolithoideae	*M. stelliferum*	54.44	41.38	3.01	0.48	0.69	—	1.32:1	0.07:1
Crusts	Corallinoideae	*B. mayae*	95.75	2.81	0.23	0.52	—	0.57	34.13:1	0.08:1
	Neogoniolithoideae	*N. frutescens*	83.37	12.12	2.13	0.42	0.06	1.89	6.88:1	0.18:1
	Lithophylloideae	*Lithophyllum* sp.	91.65	5.60	0.34	0.52	0.68	1.21	16.36:1	0.06:1
	Chamberlainoideae	*C. tumidum*	88.69	6.04	0.61	0.83	0.36	3.46	14.68:1	0.10:1
	Melobesioideae	*Lithothamnion* sp.	94.51	2.74	0.52	0.58	0.13	1.38	34.50:1	0.19:1

Table 3 Linkage analysis of genicular tissue from *C. tuberculosum*, *A. gracilis*, and *Metagoniolithon* sp.1. Units are expressed as mol%. [a]Glu = glucose, Gal = galactose, and Xyl = xylose. [b]G = β-D-galactose, LG = α-L-galactose, X = xylose, S = sulfate, U = unknown, and numbers indicate position of substitution on galactose unit

Deduced linkage[a]	Possible structural units[b]	*C. tuberculosum*	*A. gracilis*	*Metagoniolithon* sp.1
Glucose				
t-Glu	Cellulose	3.8	1.0	1.3
4-Glu	Cellulose	13.8	1.4	1.7
Galactose				
3-Gal	G	37.0	30.1	31.6
3,6-Gal	G6X, G6S	3.1	5.1	6.4
2,3,6-Gal	G2U6X, G2U6S	—	2.0	2.6
4-Gal	LG	32.4	23.4	27.3
2,4-Gal	LG2S	0.9	3.6	6.0
3,4-Gal	LG3S, G4S	2.2	—	—
2,4,6-Gal	LG2S6U	—	1.6	1.8
Xylose				
t-Xyl	G6X	0.8	4.5	3.9
Unassigned				
3-Glu	Unknown	2.3	—	—
2-Gal	Unknown	0.3	0.4	1.0
2,3-Gal	Unknown	0.7	15.4	13.8
4,6-Gal	Unknown	0.7	10.4	2.1
2-Xyl	Unknown	0.2	0.4	0.1
4-Xyl	Unknown	1.9	0.6	0.3

this is likely due to differences in extraction protocols. In the linkage analysis, the filtration step with glass wool may have removed most of the cellulose from the final sample prior to the depolymerization step. Moreover, since there was a desulfation step that may have contributed to losses, the 4-Glu that was detected likely represents residual cellulose that was not filtered out (i.e., an underestimate of total abundance).

Although D and L conformation were not tested here, it was assumed that 3-Gal units corresponded to β-D-galactose, while 4-Gal corresponded to α-L-galactose. This assumption was based on the relative proportions of 3-Gal and 4-Gal, which approached parity for all species (3-Gal:4-Gal was 1.11:1 for *C. tuberculosum*, 0.95:1 for *A. gracilis*, and 1.09:1 for *Metagoniolithon* sp.1), indicating likely involvement of these linkages in the agar backbone structure. Possible sulfation positions were not directly tested, but they were assumed to be comparable to what has been previously found in *C. cheilosporioides* (Martone et al. 2010). Overall, there was a greater proportion of galactose in *A. gracilis* and *Metagoniolithon* sp.1 compared to *C. tuberculosum*, with much of this difference being the result of galactose units with previously undocumented linkages (Table 3). 2,3-Gal was found in all three species, but it was much more abundant in *A. gracilis* and *Metagoniolithon* sp.1 than in *C. tuberculosum*. 4,6-Gal was also found in all three species, but more abundantly in *A. gracilis* than in either of the other two species. Additionally, both *A. gracilis* and *Metagoniolithon* sp.1 possessed the highly substituted units, 2,3,6-Gal and 2,4,6-Gal, neither of which was detected in *C. tuberculosum*.

The abundance of t-Xyl was roughly four times greater in *A. gracilis* and *Metagoniolithon* sp.1 than it was in *C. tuberculosum*, indicating a higher presence of terminal xylose side units on the agar backbone of these groups. For all three species, the ratio of t-Xyl to 3- and 4-Gal was much lower than the 1:3 ratio that would be expected for a typical coralline xylogalactan: roughly 1:87 for *C. tuberculosum*, 1:12 for *A. gracilis*, and 1:15 for *Metagoniolithon* sp.1.

Multivariate comparisons between tissue types and subfamilies

Monosaccharide data for all tissues were distinguished along five principal components, with the first two principal components (PC1 and PC2) accounting for 76% of the variation. PC3, PC4, and PC5 had eigenvalues < 1 and were not considered further. Contributions to PC1 were spread out amongst fucose (25%), xylose (22%), mannose (20%), galactose (18%), and rhamnose (13%).

Glucose alone contributed 53% of the variation of PC2, with lesser contributions from xylose (17%), galactose (14%), and mannose (13%). Across PC1 and PC2, crusts nested within the cluster of intergenicular tissues (Fig. 3). Clustering of calcified and uncalcified tissues was significantly different (PERMANOVA, $R^2 = 0.23$, $P < 0.001$), but the assumption of homogeneity of multivariate dispersion was violated, so at least some of this difference is due to different levels of overall variation. Based on the correlation of variables with PC1 and PC2, calcified and uncalcified tissue data seem to differ primarily in a direction correlated with galactose and xylose (Fig. 3B); this is in line with patterns seen in the monosaccharide data (Table 1).

Calcified tissues were distinguished along five principal components, with the first two principal components (PC1 and PC2) accounting for 79% of the variation. PC3, PC4, and PC5 had eigenvalues < 1 and were not considered further. Contributions to PC1 were spread out amongst glucose (26%), xylose (20%), galactose (15%), and mannose (15%). The highest contribution to PC2 was rhamnose (37%), with contributions from galactose (22%), mannose (17%), and xylose (11%). Crustose data clustered within the broader spread of intergenicular data, and metagoniolithoid intergenicula were distinct from other calcified tissues on the PC2 axis (Fig. 4). Clustering of crusts and intergenicula depended upon phylogenetic clade (PERMANOVA, Tissue Type X Clade, $R^2 = 0.17$, $P < 0.001$).

Genicular tissues were distinguished along five principal components, with the first two principal components (PC1 and PC2) accounting for 80% of the variation. PC3, PC4, and PC5 had eigenvalues < 1 and were not considered further. PC1 was mostly based on mannose (28%) and fucose (28%), with additional contributions from rhamnose (19%) and xylose (11%). PC2 was composed primarily of galactose (30%) and glucose (28%), as well as additional contributions from xylose (23%) and rhamnose (13%). Visual clustering in PC1 and PC2 was evident (Fig. 5), and this was confirmed by a significant effect of subfamily in the PERMANOVA test ($R^2 = 0.59$, $P < 0.001$). Metagoniolithoids were typically lower on the PC1 axis than most corallinoids and lithophylloids; this axis had a high contribution of mannose, which was present in all corallinoid and lithophylloid genicula, but completely absent in metagoniolithoid tissues (Table 1). Corallinoids were universally lower on the PC2 axis than either metagoniolithoids or lithophylloids (Fig. 5); this axis was highly correlated with galactose and glucose in opposite directions (Fig. 5B), which reflects the high glucose and low galactose content of corallinoids relative to other subfamilies (Table 1).

Phylogenetic signal analysis

Only PC2 had a significant phylogenetic signal for both Pagel's λ (1.00, $P < 0.01$) and Blomberg's K (1.25, $P < 0.01$). This indicates that closely related species were more similar to one another in PC2 than they were to more distantly related species (Fig. 6). No other principal components or monosaccharides had a significant phylogenetic signal (Table 4), indicating that there was no correlation between phylogeny and variation for these traits.

Correlating monosaccharides with mechanical properties

Genicula with more glucose tended to have greater breaking stress (Fig. 7A, ANOVA, $R^2 = 0.58$, $P < 0.05$); corallinoid species exhibited both the highest strength and the highest glucose content, while metagoniolithoids had the lowest strength and lowest glucose content. Genicula with greater galactose content tended to have greater breaking strain, but the trend was not significant (Fig. 7B, ANOVA, $R^2 = 0.43$, $P = 0.08$). Lithophylloid species had the highest galactose content, but not necessarily the highest breaking strain, as *Metagoniolithon* sp.2 was the most extensible species tested.

Discussion

Comparison of calcified and uncalcified tissues

Our results indicate that calcified and uncalcified coralline tissues differ significantly in their relative abundance of cellulose and matrix polysaccharides. If glucose is treated as a proxy for cellulose, then cellulose content as a percentage of dry tissue weight was variable across tissue types. However, cellulose accounted for a much larger percentage of the total polysaccharide content in calcified tissues. Similarly, if galactose is treated as a proxy for galactans, then galactans were much more abundant in uncalcified tissues than in calcified tissues, both in dry weight and percentage of polysaccharide content. Overall, this suggests that differences in the relative abundance of cellulose and matrix polysaccharides are driven by greater galactan content in uncalcified tissues, rather than greater cellulose content in calcified tissues.

While we were able to demonstrate that calcified tissues have some broad similarity in chemical composition, we did not detect higher xylose abundance expected in calcified tissues compared to uncalcified tissues. Xylose content was actually higher overall

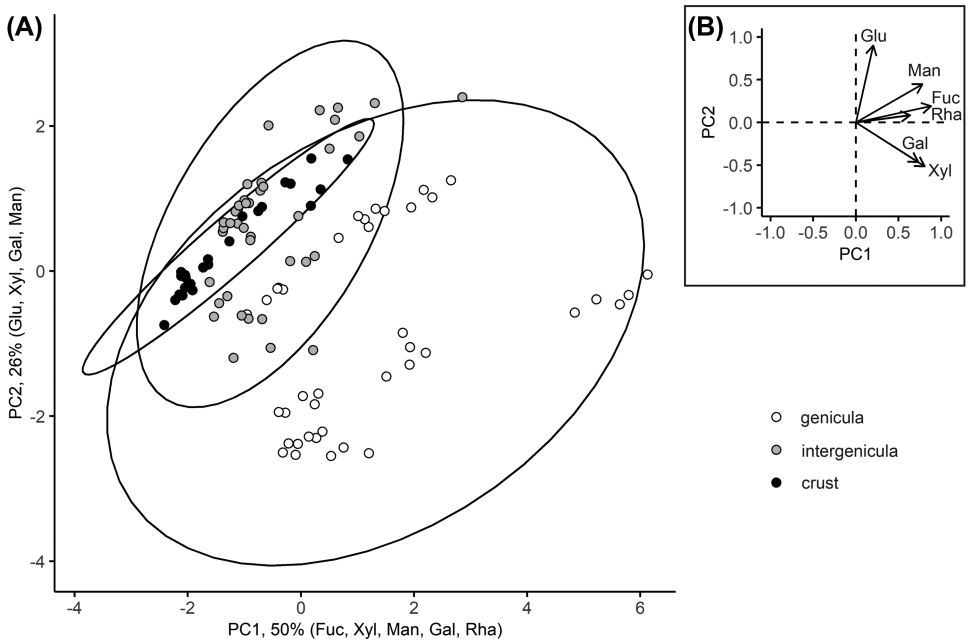

Fig. 3 The first two principal components of a PCA run on neutral monosaccharide data from genicula, intergenicula, and crusts. The first principal component (PC1) is composed primarily of fucose (25%), xylose (22%), mannose (20%), galactose (18%), and rhamnose (13%), where % indicates contribution to PC1 specifically. The second principal component (PC2) is composed primarily of glucose (53%), xylose (17%), galactose (14%), and mannose (13%), where % indicates contribution to PC2 specifically. All other contributions to PC1 and PC2 are < 10%. (**A**) Each circle represents a single sample, and color indicates whether the sample is genicula (white), intergenicula (gray), or crust (black). Ellipses indicate 95% CI around tissue type clusters. (**B**) Correlation of variables with PC1 and PC2. Arrow angle indicates approximate correlation, and arrow length indicates variable variance.

in most uncalcified tissues (with the exception of the genicula of *C. tuberculosum*), and the relative proportions of xylose and galactose did not show a consistent pattern based on tissue type. The results of the linkage analysis, however, indicate that not all xylose found in genicula is necessarily associated with xylogalactans. The only previous study to analyze genicular tissue in isolation specifically analyzed galactan extracts (Martone et al. 2010), while we analyzed whole hydrolyzed tissue. The higher xylose content of genicula in this study compared to that found by Martone et al. (2010) suggests that 2-Xyl and 4-Xyl are associated with polysaccharides other than galactans. Furthermore, the ratio of t-Xyl (the linkage previously associated with xylogalactans) to 3- and 4-Gal in genicular tissues was universally lower than the 1:3 ratio suggested by Cases et al. (1992, 1994). Based on these results, genicular tissues are indeed very low in xylogalactan content (or genicular xylogalactans have low numbers of xylose side-chains) relative to what has previously been observed in corallines (Turvey and Simpson 1965; Cases et al. 1992, 1994; Usov et al. 1995, 1997; Takano et al. 1996; Navarro and Stortz 2002, 2008; Navarro et al. 2011), consistent with the hypothesis of Martone et al.(2010) that stripping xylose side-chains from galactans may contribute to the disruption of calcification.

Table 4 Statistical testing for phylogenetic signal of chemical traits of calcified tissues

Trait	Blomberg's κ	*P*-value	Pagel's λ	*P*-value
PC1	0.51	0.53	0.00	1.00
PC2	1.25	< 0.01	1.00	< 0.01
PC3	0.33	0.88	0.00	1.00
PC4	0.64	0.24	0.09	0.87
PC5	0.50	0.52	0.00	1.00
Fucose	0.43	0.72	0.00	1.00
Rhamnose	0.39	0.78	0.26	0.45
Galactose	0.73	0.16	0.66	0.16
Glucose	0.49	0.60	0.00	1.00
Xylose	0.57	0.42	0.00	1.00
Mannose	0.89	0.06	1.00	0.21

While the surprisingly high xylose content in genicular tissues may be explained by the presence of different xylose-containing polysaccharides, the ratio of xylose:galactose was still lower than the expected 1:3 for most calcified tissues. As we did not perform linkage analysis on calcified tissues, we could not determine the

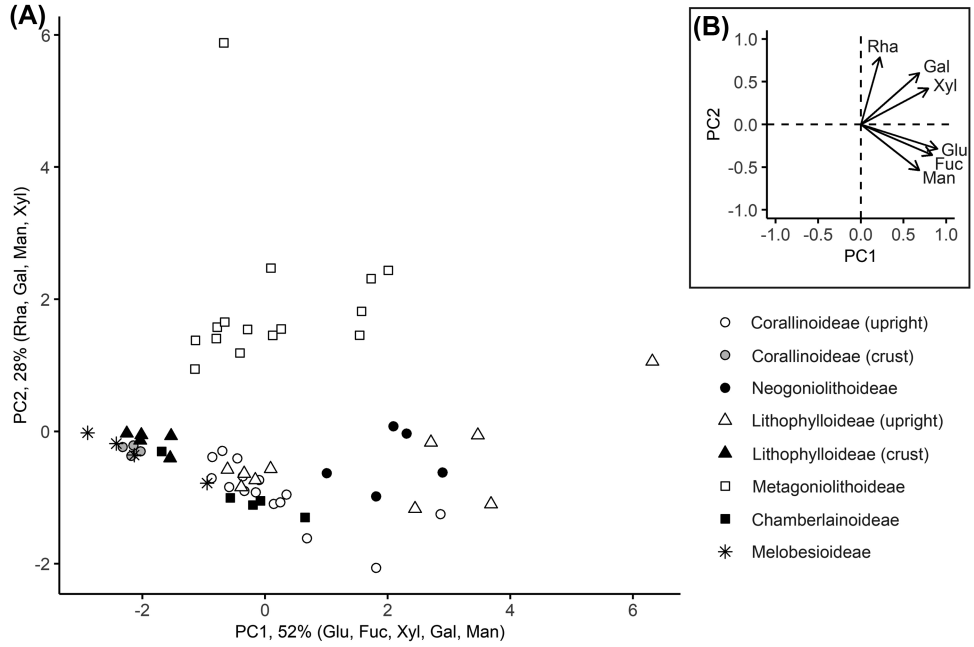

Fig. 4 The first two principal components of a PCA run on neutral monosaccharide data from calcified tissues of articulated and crustose corallines. The first principal component (PC1) is composed primarily of glucose (26%), xylose (20%), galactose (15%), and mannose (15%), where % indicates contribution to PC1 specifically. The second principal component (PC2) is composed primarily of rhamnose (37%), galactose (22%), mannose (17%), and xylose (11%), where % indicates contribution to PC2 specifically. All other contributions to PC1 and PC2 are $< 10\%$. (**A**) Each point represents a single sample. Shape indicates close relatedness between subfamilies, and color indicates whether a group is articulated (white), crustose (black), or a crust that has evolved from an articulated species (gray). Corallinoideae (articulated) includes *C. tuberculosum*, *C. chilensis*, and *J. macmillanii*; Corallinoideae (crust) includes *B. mayae*; Neogoniolithoideae (black circles) includes *N. frutescens*; Lithophylloideae (articulated) includes *A. gracilis* and *Amphiroa* sp.; Lithophylloideae (crust) includes *ithophyllum* sp.; Metagoniolithoideae includes *Metagoniolithon* sp.1, *Metagoniolithon* sp.2, and *M. stelliferum*; and Melobesioideae includes the basal crustose species *Lithothamnion* sp. (**B**) Correlation of variables with PC1 and PC2. Arrow angle indicates approximate correlation, and arrow length indicates variable variance.

ratio of t-Xyl to 3- and 4-Gal specifically. Future work on galactans of articulated corallines should include separate linkage analysis of calcified and uncalcified tissues, in order to better compare the abundance of specific polysaccharides such as xylogalactans.

Comparison of crustose and intergenicular tissues

While crustose and articulated species were chemically distinct from one another within a given clade, the way in which they differed was not consistent across a broader spread of species. Moreover, chemical differences between articulated taxa and crusts within each clade could reflect phylogenetic relatedness more so than morphology, since chemically similar articulated species were also more closely related to one another than to the next most closely related crust. PCA results of the highly derived corallinoid crust *B. mayae* (which evolved from articulated ancestors) further support this conclusion, as this species clustered more closely with corallinoid intergenicula than it did with the crustose sister taxon *N. frutescens*.

The connection between ancestral history and chemistry in calcified tissues is unclear and warrants further investigation. While phylogenetic signal analysis indicated that PC2 of calcified tissues was more similar in closely related species, this appeared to be largely driven by segregation of metagoniolithoid intergenicula apart from all other calcified tissues. None of the monosaccharides that contributed to PC2 had a significant phylogenetic signal on their own, suggesting it is the combination that is important in distinguishing metagoniolithoids from the other taxa. Linkage analysis of metagoniolithoid intergenicula would help to determine whether these sugars (rhamnose, galactose, mannose, and xylose) are clustered in some unusual way in this clade.

Chemical divergence of genicular cell walls

Results from this study demonstrate that genicula have evolved along different trajectories with respect to chemical composition, which likely also explains their distinct material properties. Glucose abundance was generally higher in corallinoid genicula than

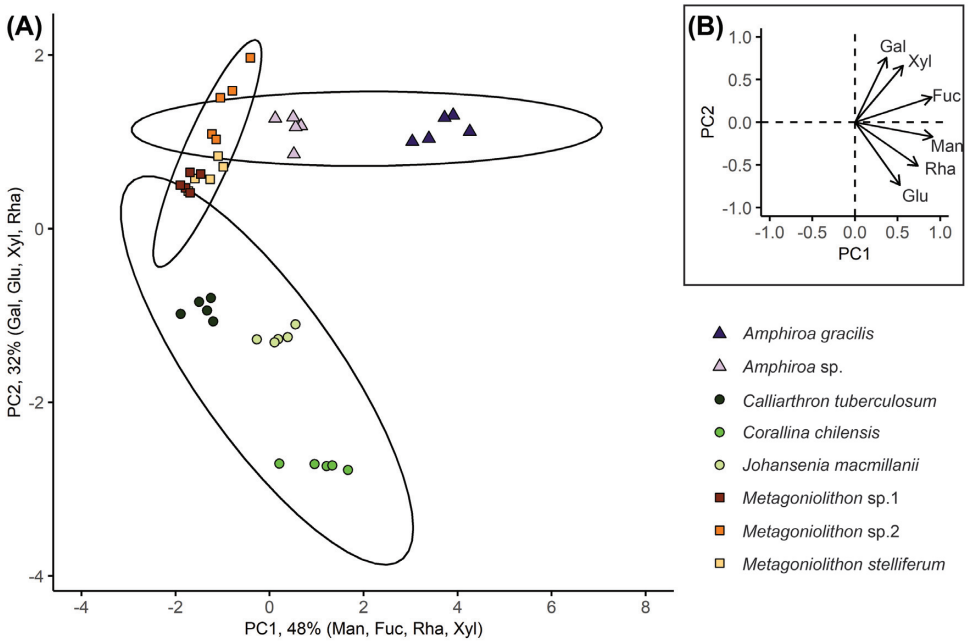

Fig. 5 The first two principal components of a PCA run on neutral monosaccharide data from genicula of articulated corallines. The first principal component (PC1) is composed primarily of mannose (28%), fucose (28%), rhamnose (19%), and xylose (11%), where % indicates contribution to PC1 specifically. The second principal component (PC2) is composed primarily of galactose (30%), glucose (28%), xylose (23%), and rhamnose (13%), where % indicates contribution to PC2 specifically. All other contributions to PC1 and PC2 are $< 10\%$. (**A**) Each point represents a single sample. Shapes indicate subfamily (Corallinoideae = circles, Lithophylloideae = triangles, and Metagoniolithoideae = squares). Species within a subfamily are differentiated by shade. Ellipses indicate 95% CI around subfamilies. (**B**) Correlation of variables with PC1 and PC2. Arrow angle indicates approximate correlation, and arrow length indicates variable variance.

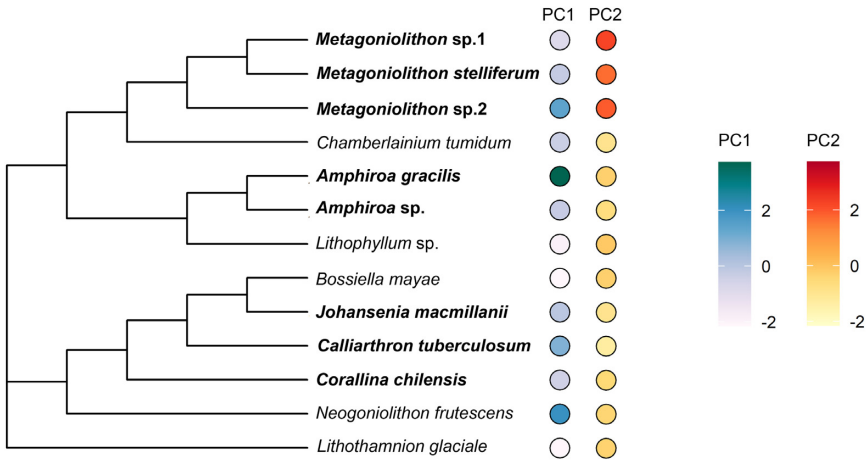

Fig. 6 Phylogenetic distribution of the first two principal components of a PCA run on neutral monosaccharide data from calcified tissues. Articulated species are bolded. There is no significant phylogenetic signal for PC1, but there is a significant phylogenetic signal for PC2 (Blomberg's $\kappa = 1.25, P < 0.01$; Pagel's $\lambda = 1.00, P < 0.01$).

in lithophylloid and metagoniolithoid genicula, and linkage analysis indicated that much of the glucose in genicular tissues originated from cellulose. Therefore, the strong correlation between glucose abundance and material strength implies that cellulose has a structural role in resisting tensile forces in the cell walls of coralline genicula, particularly in corallinoids. These results are consistent with Martone et al. (2019), who found that the genicula of *C. tuberculosum* became significantly stronger with the addition of cellulose-rich secondary cell walls. Corallinoid genicula are composed of a single tier of elongated cells that are typically ~0.5 mm in length or less, while the multi-tiered genicula of many lithophylloids and metagoniolithoids

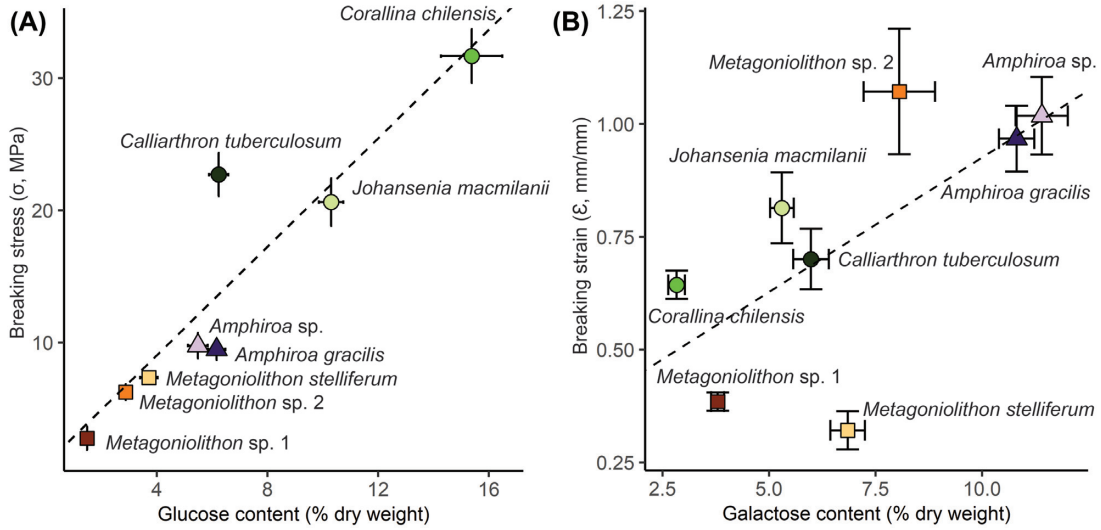

Fig. 7 Correlations between (**A**) glucose content and tissue breaking stress ($P < 0.01$), and (**B**) galactose content and tissue breaking strain ($P = 0.08$) in genicular tissue of articulated corallines. Points represent species averages and error bars represent SEM. Material properties and monosaccharide content were measured on different sample sets. Shapes indicate subfamily (Corallinoideae = circles, Lithophylloideae = triangles, and Metagoniolithoideae = squares). Species within a subfamily are differentiated by shade. Black dotted lines represent lines of best fit (**A**: $y = 2.05x + 0.58$; **B**: $y = 0.06x + 0.33$)

regularly exceed lengths of 1 mm and beyond (Johansen 1981; Janot and Martone 2018)—as a result of this difference in length, corallinoid genicula are subject to a higher degree of stress during bending (Janot and Martone 2018). If genicular length is uniquely developmentally constrained in corallinoids, then cellulose-rich secondary cell walls might have evolved in response to selective pressure to withstand increased stress.

While a combination of monosaccharide and linkage analysis indicated differences in overall galactan abundance in the genicula of corallinoids, lithophylloids, and metagoniolithoids, linkage analysis also revealed differences in galactan structure. Of note were two sugars present in *A. gracilis* and *Metagoniolithon* sp.1, but absent in *C. tuberculosum*: 2,3,6-Gal and 2,4,6-Gal. If these units are part of the galactan structure, they indicate a higher degree of branching in the galactans of lithophylloid and metagoniolithoid genicula compared to those of corallinoid genicula. This level of branching would also be higher than what has been previously described in coralline galactans. While results of this study indicated an interesting but insignificant trend between galactan content and extensibility, the impact of galactan branching on material properties is largely unexplored and could mask any effect of total abundance.

Summary

This work is the first to compare the chemical composition of genicula and intergenicula across all three articulated subfamilies, as well as the first to make direct comparisons between calcified tissues of crustose and articulated species. It offers a new perspective on the unifying chemistry of calcified coralline cell walls, as well as the convergent evolution of coralline genicula. The results suggest that chemical composition of calcified tissues across both articulated and crustose clades are broadly similar, perhaps due to their shared structural role. In contrast, genicular tissues of articulated taxa from different articulated clades exhibit several notable differences in both content and structure of cell wall polysaccharides, further emphasizing that the repeated evolution of jointed morphologies in corallines has proceeded along multiple biochemical and developmental pathways.

Acknowledgments

We would like to express our gratitude to the Heiltsuk Nation, Wuikinuxv Nation, and Pacheedaht Nation for their stewardship of the land and water in the local area. Collections on Calvert Island, BC were supported by the Hakai Institute and Tula Foundation. Collections from Botanical Beach, BC were performed under a park use permit provided by the Ministry of Environment (Parks and Protected Areas Division, Vancouver Island Region, permit no. 104149). Collections in Moorea, French Polynesia were completed under permits issued to Robert Carpenter by the French Polynesian Government (Délégation à la Recherche) and the Haut-Commissariat de la République en Polnésie Française

(DTRT). Collections in Western Australia were performed under licenses provided by Department of Environment and Conservation of the Government of Western Australia (SW015180, SW015181, and SW015182 in 2012; SW015966 in 2014), as well as a Regulation 4 Lawful Authority notice for Shoalwater Islands Marine Park (Point Peron).

We are immensely thankful to Rachael Wade, Brenton Twist, and Jasmine Lai for their assistance and expertise in sequencing. Additional thanks are due to Rachael for scanning herbarium specimens for Fig. 2, as well as Beau Gravlin for his illustrations in Fig. 1. We are also grateful to Mark Denny, John Huisman, Gary Kendrick, and John Statton for providing assistance in the collection of Australian coralline specimens, and to Robert Carpenter and Sarah Merolla for providing us with specimens of *Neogoniolithon frutescens*. Finally, we would like to acknowledge the invaluable feedback of Lauran Liggan, Sam Starko, Liam Coleman, Matthew Whalen, and Matthew Lemay at various stages of this project.

Funding

This work was supported by funding provided by the National Sciences and Engineering Research Council (NSERC) *via* a Discovery Grant to P.T.M., as well as a graduate fellowship to K.J. Support was also provided by the Phycological Society of America and the Beaty Biodiversity Research Centre to K.J., and additional travel funds were provided by a National Science Foundation (NSF) grant to Mark W. Denny (IOS-1052161). The linkage analysis was supported by a grant from the Chemical Sciences, Geosciences and Biosciences Division, Office of Basic Energy Sciences, US Department of Energy, to Parastoo Azadi at the Complex Carbohydrate Research Center (DE-SC0015662).

Supplementary data

Supplementary data available at *ICB* online.

Data availability

Data not otherwise provided in this article or in the online supplementary material will be shared on reasonable request to the corresponding author.

References

Aguirre J, Perfectti F, Braga JC. 2010. Integrating phylogeny, molecular clocks, and the fossil record in the evolution of coralline algae (Corallinales and Sporolithales, Rhodophyta). Paleobiology 36:519–33.

Altschul SF, Madden TL, Schäffer AA, Zhang J, Zhang Z, Miller W, Lipman DJ. 1997. Gapped BLAST and PSI-BLAST: a new generation of protein database search programs. Nucleic Acids Res 25:3389–402.

Bailey JC, Chapman RL. 1998. A phylogenetic study of the Corallinales (Rhodophyta) based on nuclear small-subunit rRNA gene sequences. J Phycol 34:692–705.

Bilan MI, Usov AI. 2001. Polysaccharides of calcareous algae and their effect on the calcification process. Russ J Bioorg Chem 27:2–16.

Bittner L, Payri CE, Maneveldt GW, Couloux A, Cruaud C, de Reviers B, Le Gall L. 2011. Evolutionary history of the Corallinales (Corallinophycidae, Rhodophyta) inferred from nuclear, plastidial and mitochondrial genomes. Mol Phylogenet Evol 61:697–713.

Boller ML, Carrington E. 2006. The hydrodynamic effects of shape and size change during reconfiguration of a flexible macroalga. J Exp Biol 209:1894–903.

Burgert I. 2006. Exploring the micromechanical design of plant cell walls. Am J Bot 93:1391–401.

Calcagno V. 2020. Glmulti: model selection and multimodel inference made easy. R package version 1.0.8. https://CRAN.R-project.org/package=glmulti.

Carrington E, Grace SP, Chopin T. 2001. Life history phases and the biomechanical properties of the red alga *Chondrus crispus* (Rhodophyta). J Phycol 37:699–704.

Cases MR, Stortz CA, Cerezo AS. 1992. Methylated, sulphated xylogalactans from the red seaweed *Corallina officinalis*. Phytochemistry 31:3897–900.

Cases MR, Stortz CA, Cerezo AS. 1994. Structure of the 'corallinans'—sulfated xylogalactans from *Corallina officinalis*. Int J Biol Macromol 16:93–7.

Darriba D, Taboada GL, Doallo R, Posada D. 2012. jModelTest 2: more models, new heuristics and parallel computing. Nat Methods 9:772.

Denny M, Gaylord B. 2002. The mechanics of wave-swept algae. J Exp Biol 205:1355–62.

Ducker SC. 1979. The genus *Metagoniolithon* Weber-van Bosse (Corallinaceae, Rhodophyta). Aust J Bot 27:67–101.

Frei E, Preston RD. 1961. Variants in the structural polysaccharides of algal cell walls. Nature 192:939–43.

Genet M, Stokes A, Salin F, Mickovski SB, Fourcaud T, Dumail J-F, van Beek R. 2005. The influence of cellulose content on tensile strength in tree roots. Plant Soil 278:1–9.

Girault R, Bert F, Rihouey C, Jauneau A, Morvan C, Jarvis M. 1997. Galactans and cellulose in flax fibres: putative contributions to the tensile strength. Int J Biol Macromol 21:179–88.

Hale BB. 2001. Macroalgal materials: foiling fracture and fatigue from fluid forces [dissertation]. [Stanford (CA)]: Stanford University.

Harder DL, Speck O, Hurd CL, Speck T. 2004. Reconfiguration as a prerequisite for survival in highly unstable flow-dominated habitats. J Plant Growth Regul 23:98–107.

Heiss C, Stacey Klutts J, Wang Z, Doering TL, Azadi P. 2009. The structure of *Cryptococcus neoformans* galactoxylomannan contains β-d-glucuronic acid. Carbohydr Res 344:915–20.

Hind KR, Gabrielson PW, Jensen C, Martone PT. 2018. Evolutionary reversals in *Bossiella* (Corallinales, Rhodophyta): first report of a coralline genus with both geniculate and nongeniculate species. J Phycol 54:788–98.

Hind KR, Gabrielson PW, Jensen CP, Martone PT. 2016. Crusticorallina gen. nov., a nongeniculate genus in the subfamily Corallinoideae (Corallinales, Rhodophyta). J Phycol 52:929–41.

Huntley SK, Ellis D, Gilbert M, Chapple C, Mansfield SD. 2003. Significant increases in pulping efficiency in C4H-F5H-transformed poplars: improved chemical savings and reduced environmental toxins. J Agric Food Chem 51:6178–83.

Husson F, Josse J, Lê S. 2008. FactoMineR: an R package for multivariate analysis. J Stat Softw 25:1–18.

Janot K, Martone PT. 2016. Convergence of joint mechanics in independently-evolving, articulated coralline algae. J Exp Biol 219:383–91.

Janot KG, Martone PT. 2018. Bending strategies of convergently evolved, articulated coralline algae. J Phycol 54:305–16.

Johansen HW. 1969. Patterns of genicular development in *Amphiroa* (Corallinaceae). J Phycol 5:118–23.

Johansen HW. 1981. Coralline algae: a first synthesis. Boca Raton (FL): CRC Press. p. 249.

Kassambara A, Mundt F. 2020. Factoextra: extract and visualize the results of multivariate data analyses. R package version 1.0.7. https://CRAN.R-project.org/package=factoextra.

Kato A, Baba M, Suda S. 2011. Revision of the Mastophoroideae (Corallinales, Rhodophyta) and polyphyly in nongeniculate species widely distributed on Pacific coral reefs. J Phycol 47:662–72.

Kearse M, Moir R, Wilson A, Stones-Havas S, Cheung M, Sturrock S, Buxton S, Cooper A, Markowitz S, Duran C et al. 2012. Geneious basic: an integrated and extendable desktop software platform for the organization and analysis of sequence data. Bioinformatics 28:1647–9.

Kloareg B, Quatrano RS. 1988. Structure of the cell walls of marine algae and ecophysiological functions of the matrix polysaccharides. Oceanogr Mar Biol Annu Rev 26:259–315.

Kraemer GP, Chapman DJ. 1991. Biomechanics and alginic acid composition during hydrodynamic adaptation by *Egregia menziesii* (Phaeophyta) juveniles. J Phycol 27:47–53.

Kumar S, Stecher G, Li M, Knyaz C, Tamura K. 2018. MEGA X: molecular evolutionary genetics analysis across computing platforms. Mol Biol Evol 35:1547–9.

Kundal P. 2011. Generic distinguishing characteristics and stratigraphic ranges of fossil corallines: an update. J Geol Soc India 78:571–86.

Martone PT. 2006. Size, strength and allometry of joints in the articulated coralline *Calliarthron*. J Exp Biol 209:1678–89.

Martone PT, Denny MW. 2008. To bend a coralline: effect of joint morphology on flexibility and stress amplification in an articulated calcified seaweed. J Exp Biol 211:3421–32.

Martone PT, Janot K, Fujita M, Wasteneys G, Ruel K, Joseleau J-P, Estevez JM. 2019. Cellulose-rich secondary walls in wave-swept red macroalgae fortify flexible tissues. Planta 250:1867–79.

Martone PT, Kost L, Boller M. 2012. Drag reduction in wave-swept macroalgae: alternative strategies and new predictions. Am J Bot 99:806–15.

Martone PT, Navarro DA, Stortz CA, Estevez JM. 2010. Differences in polysaccharide structure between calcified and uncalcified segments in the coralline *Calliarthron cheilosporioides* (Corallinales, Rhodophyta). J Phycol 46:507–15.

Masarin F, Cedeno FRP, Chavez EGS, de Oliveira LE, Gelli VC, Monti R. 2016. Chemical analysis and biorefinery of red algae *Kappaphycus alvarezii* for efficient production of glucose from residue of carrageenan extraction process. Biotechnol Biofuels 9:122.

Navarro DA, Ricci AM, Rodríguez MC, Stortz CA. 2011. Xylogalactans from *Lithothamnion heterocladum*, a crustose member of the Corallinales (Rhodophyta). Carbohydr Polym 84:944–51.

Navarro DA, Stortz CA. 2002. Isolation of xylogalactans from the Corallinales: influence of the extraction method on yields and compositions. Carbohydr Polym 49:57–62.

Navarro DA, Stortz CA. 2008. The system of xylogalactans from the red seaweed *Jania rubens* (Corallinales, Rhodophyta). Carbohydr Res 343:2613–22.

Okazaki M, Furuya K, Tsukayama K, Nisizawa K. 1982. Isolation and identification of alginic acid from a calcareous red alga *Serraticardia maxima*. Botan Mar 25:123–31.

Okazaki M, Tazawa K. 1989. Alginic acid in Corallinaceae (Cryptonemiales, Rhodophyta). ALGAE 4:213–9.

Oksanen J, Blanchet FG, Friendly M, Kindt R, Legendre P, McGlinn D, Minchin PR, O'Hara RB, Simpson GL, Solymos P et al. 2020. Vegan: community ecology package. R package version 2.5.7. https://CRAN.R-project.org/package=vegan.

R Core Team. 2021. R: a language and environment for statistical computing. Vienna: R Foundation for Statistical Computing. https://www.R-project.org/.

Ratnasingham S, Hebert PDN. 2007. bold: the Bbrcode of life data system (http://www.barcodinglife.org). Mol Ecol Notes 7:355–64.

Rees DA, Conway E. 1962. The structure and biosynthesis of porphyran: a comparison of some samples. Biochem J 84:411–6.

Revell LJ. 2012. phytools: an R package for phylogenetic comparative biology (and other things). Methods Ecol Evol 3:217–23.

RStudio Team. 2021. RStudio: Integrated development environment for R. Boston (MA): RStudio, PBC. https://rstudio.com.

Saunders GW, McDevit DC. 2012. Methods for DNA barcoding photosynthetic protists emphasizing the macroalgae and diatoms. Methods Mol Biol 858:207–22.

Sayers EW, Cavanaugh M, Clark K, Ostell J, Pruitt KD, Karsch-Mizrachi I. 2020. GenBank. Nucleic Acids Res 48:D84–86.

Starko S, Mansfield SD, Martone PT. 2018. Cell wall chemistry and tissue structure underlie shifts in material properties of a perennial kelp. Eur J Phycol 53:307–17.

Steneck RS. 1986. The ecology of coralline algal crusts: convergent patterns and adaptative strategies. Annu Rev Ecol Syst 17:273–303.

Takano R, Hayashi J, Hayashi K, Hara S, Hirase' S. 1996. Structure of a water-soluble polysaccharide sulfate from the red seaweed *Joculator maximus* Manza. Botan Mar 39:95–102.

Turvey JR, Simpson PR. 1965. Polysaccharides from *Corallina officinalis*. Proc Int Seaweed Symp 5:323–7.

Usov AI. 1992. Sulfated polysaccharides of the red seaweeds. Food Hydrocolloids 6:9–23.

Usov AI, Bilan MI, Klochkova NG. 1995. Polysaccharides of algae. 48. polysaccharide composition of several calcareous red algae: isolation of alginate from *Corallina pilulifera* P. *et* R. (Rhodophyta, Corallinaceae). Botan Mar 38:43–51.

Usov AI, Bilan MI, Shashkov AS. 1997. Structure of a sulfated xylogalactan from the calcareous red alga *Corallina pilulifera* P. *et* R. (Rhodophyta, Corallinaceae). Carbohydr Res 303:93–102.